

# Two 3D chiral coordination polymers with 4-connected 6<sup>6</sup> topological net: synthesis, structure and magnetic properties†

Zheng-Bo Han,<sup>\*a</sup> Jian-Wei Ji,<sup>a</sup> Hai-Yan An,<sup>\*b</sup> Wei Zhang,<sup>a</sup> Guang-Xi Han,<sup>a</sup> Guo-Xin Zhang<sup>a</sup> and Li-Guo Yang<sup>c</sup>

Received 7th May 2009, Accepted 22nd August 2009

First published as an Advance Article on the web 11th September 2009

DOI: 10.1039/b909083e

The hydrothermal reaction of Co(II)/Cu(II), 5-hydroxyisophthalic acid and dipyrindophenazine leads to the generation of two 3D chiral coordination polymers, [M(hip)(DPPZ)]<sub>n</sub> (M = Co(1), Cu(2), H<sub>2</sub>hip = 5-hydroxyisophthalic acid, DPPZ = dipyrindophenazine), which contain M-hip-M helical chains (M = Co, Cu) and possess a new four-connected 6<sup>6</sup> topological net. The resulting crystals were not a racemic mixture but an enantiomeric excess, which was confirmed by the measurement of optical rotation of the bulk samples using solid state vibrational circular dichroism (VCD) and solid circular dichroism (CD) based on the large crystals from one crystallization. The magnetic properties of **1** and **2** have been investigated by variable-temperature magnetic susceptibility and magnetization measurements, and the results reveal that antiferromagnetic interactions exist in **1** and **2**.

## Introduction

The design and synthesis of chiral metal–organic frameworks (MOFs) has attracted much attention in coordination chemistry, not only because of their intriguing variety of architectures and topologies but also owing to their potential applications in nonlinear optical (NLO) materials, asymmetric catalysis and chiral separations.<sup>1–2</sup> Several approaches have been previously reported for constructing chiral MOFs, including the introduction of chiral ligands,<sup>3</sup> the influence of chiral templates or the chiral physical environment,<sup>4</sup> and spontaneous resolution without any chiral auxiliary.<sup>5</sup> Among them, the main synthetic strategy to generate an enantiopure material has been the use of chiral ligands because spontaneous resolution from achiral starting materials only occurs occasionally and the products are normally a racemic mixture of chiral crystals, although each crystal is a single enantiomer.<sup>6</sup> While the use of enantiopure ligands leads to the generation of a single enantiomeric product. To date, many chiral coordination polymers have been obtained, while there are only a few examples of spontaneous resolution, in which the chiral information in the building units can be transmitted into a higher dimensionality to generate chiral coordination polymers.<sup>7</sup>

Towards the goal of designing chiral materials, we are currently undertaking a self-assembly approach between transition metal ions and V-shaped dicarboxylates, for example, the 5-hydroxyisophthalic acid ligand. Herein we report two novel

3D chiral coordination polymers, [Co(hip)(DPPZ)]<sub>n</sub> (**1**) and [Cu(hip)(DPPZ)]<sub>n</sub> (**2**), constructed from two achiral organic ligands, 5-hydroxyisophthalic acid (H<sub>2</sub>hip) and dipyrindophenazine (DPPZ).

## Experimental

### Materials and methods

All reagents and solvents employed were commercially available and used without further purification. The C, H, and N microanalyses were carried out with a Perkin-Elmer 240 elemental analyzer. The FT-IR spectra were recorded from KBr pellets in the range 4000–400 cm<sup>-1</sup> on a Nicolet 5DX spectrometer. X-ray powder diffraction (XPRD) data were recorded with a Rigaku D/max 2200 vpc diffractometer with Cu-Kα radiation (λ = 1.5406 Å). VCD spectra were measured with the Bruker PMA 37 spectrometer (resolution: 4 cm<sup>-1</sup>; zero filling factor: 2; scan time: 3 h). Circular dichroism spectra were measured using a JASCO J-810 spectropolarimeter. Spectra were collected on powder samples of a crystal embedded in KBr pellets between 200 and 300 nm at a speed of 100 nm min<sup>-1</sup>. Variable-temperature magnetic susceptibility data were obtained on a SQUID magnetometer (Quantum Design, MPMS-7) in the temperature range 2–300 K with an applied field of 10 KG.

### Hydrothermal syntheses.

[Co(Hip)(DPPZ)]<sub>n</sub> (**1**). A reaction mixture of Co(NO<sub>3</sub>)<sub>2</sub>·6H<sub>2</sub>O (0.5 mmol, 0.145 g), H<sub>2</sub>hip (0.5 mmol, 0.091 g), DPPZ (0.5 mmol, 0.144 g), NaOH (0.5 mmol, 0.02 g) and H<sub>2</sub>O (10 ml) was stirred for 20 min in air, then transferred and sealed in a 18-mL Teflon<sup>TM</sup>-lined autoclave, which was heated to 453 K for 72 h, followed by slow cooling (5 K h<sup>-1</sup>). The resulting light purple block crystals were washed with distilled water and dried in air (yield: ca. 45%). Elemental analysis calcd (%) for **1** C<sub>26</sub>H<sub>14</sub>CoN<sub>4</sub>O<sub>5</sub>: C, 59.90; H, 2.71; N, 10.75 Found: C, 59.88; H, 2.73; N, 10.68%. IR (KBr Pellets, cm<sup>-1</sup>): 1607 (m), 1551 (s),

<sup>a</sup>College of Chemistry, Liaoning University, Shenyang, 110036, P. R. China. E-mail: ceshzb@lnu.edu.cn; Fax: (+86) 24-62202380; Tel: (+86) 24-62207849

<sup>b</sup>Department of Chemistry, Dalian University of Technology, Dalian, 116023, P. R. China. E-mail: anhy@dlut.edu.cn

<sup>c</sup>Alan G. MacDiarmid Institute, Jilin University, Changchun, 130012, P. R. China

† Electronic supplementary information (ESI) available: TGA curve, and simulated and experimental X-ray powder diffraction patterns for **1** and **2**. CCDC reference numbers 714701 (**2**) & 714702 (**1**). For ESI and crystallographic data in CIF or other electronic format see DOI: 10.1039/b909083e

1495 (s), 1447 (s), 1411 (w), 1384 (vs), 1357 (s), 1297 (s), 1282 (s), 1219 (w), 1076 (w), 818 (w), 782 (s), 734 (w).

$[Cu(hip)(DPPZ)]_n$  (**2**). Synthesis of **2** was similar to that of **1** using  $Cu(NO_3)_2 \cdot 3H_2O$  (0.120 g, 0.5 mmol) instead of  $Co(NO_3)_2 \cdot 6H_2O$ . The resulting green block crystals were washed with distilled water and dried in air (yield: ca. 30%). Elemental analysis calcd (%) for **2**  $C_{26}H_{14}CuN_4O_5$ : C, 59.37; H, 2.68; N, 10.65. Found: C, 59.48; H, 2.82; N, 10.85%. IR (KBr Pellets,  $cm^{-1}$ ): 1606 (m), 1548 (s), 1497 (s), 1441 (s), 1407 (w), 1384 (vs), 1357 (s), 1295 (s), 1281 (s), 1216 (w), 1076 (w), 818 (w), 784 (s), 731 (w).

**X-ray crystallography.** Single-crystal X-ray diffraction measurements were carried out on a Bruker P4 diffractometer at room temperature. The data collections were performed with Mo-K $\alpha$  radiation ( $\lambda = 0.71073 \text{ \AA}$ ). Unit cell dimensions were obtained with least squares refinements, and all structures were solved by direct methods. The non-hydrogen atoms were located in successive difference Fourier syntheses. The final refinement was performed by full matrix least squares methods with anisotropic thermal parameters for non-hydrogen atoms on  $F^2$ .<sup>8</sup> Crystallographic data and experimental details for structural analyses are summarized in Table 1, and selected bond lengths and angles are listed in Table 2.

## Results and discussion

Single-crystal X-ray analysis has revealed that **1** and **2**, crystallizing in the chiral space group  $P4_32_12$ , are isomorphous, infinite 3D chiral coordination polymers. So only the structure of **1** is described here. There is one crystallographically independent Co centre, one DPPZ and one hip ligand in the asymmetric unit. Each Co centre is five-coordinate and surrounded by three oxygen atoms from three different hip ligands and two nitrogen atoms from the DPPZ ligands (Co(1)–O(4A) 1.970(2), Co(1)–O(2) 2.014(2), Co(1)–O(1B) 2.017(2)  $\text{\AA}$ , Co(1)–N(1) 2.145(2) and Co(1)–N(2) 2.107(2)). Thus, all Co centres display distorted quadrangular pyramidal coordination geometries with the O–Co–O angles ranging from 93.60(10) to 99.36(9) $^\circ$  and the N–Co–O angles from 86.71(9)–164.97(9) $^\circ$ . As shown in Fig. 1, two Co(DPPZ) moieties are linked by four hip ligands to form a binuclear  $[Co_2(DPPZ)_2(hip)_4]^{4+}$  second building unit (SBU). Two

**Table 1** Crystallographic data and structural refinement summary for **1** and **2**

	<b>1</b>	<b>2</b>
chem. form	$C_{26}H_{14}CoN_4O_5$	$C_{26}H_{14}CuN_4O_5$
form wt	521.34	525.95
cryst syst	Tetragonal	Tetragonal
space group	$P4_32_12$	$P4_32_12$
$a/\text{\AA}$	11.600(2)	11.624(2)
$b/\text{\AA}$	11.600(2)	11.624(2)
$c/\text{\AA}$	31.419(2)	30.720(8)
$V/\text{\AA}^3$	4228.0(10)	4150.6(15)
$T/K$	293	293
$D_c/g\text{ cm}^{-3}$	1.638	1.683
$Z$	8	8
$\mu(\text{Mo-K}\alpha)/\text{mm}^{-1}$	0.863	1.104
no. unique data ( $R_{int}$ )	4849 (0.0357)	4093 (0.0724)
no. total reflns	6668	5721
$R_1^a/wR_2^b$	0.0370/0.0880	0.0480/0.1193

<sup>a</sup>  $R_1 = \sum \|F_o\| - |F_c|/\sum \|F_o\|$ ; <sup>b</sup>  $wR_2 = \sum [w(F_o^2 - F_c^2)^2]/\sum [w(F_o^2)^2]^{1/2}$ .

**Table 2** Selected bond distances and angles for **1** and **2**

Bond	$D$ ( $\text{\AA}$ )	Angle ( $^\circ$ )	$\omega$ ( $^\circ$ )
<b>1</b>			
Co(1)–O(4A)	1.970(2)	O(4A)–Co(1)–O(2)	99.36(9)
Co(1)–O(2)	2.014(2)	O(4A)–Co(1)–N(2)	118.66(10)
Co(1)–O(1B)	2.017(2)	O(2)–Co(1)–O(1B)	93.60(10)
Co(1)–N(1)	2.145(2)	O(2)–Co(1)–N(2)	140.32(10)
Co(1)–N(2)	2.107(2)	O(1B)–Co(1)–N(2)	93.80(9)
		N(1)–Co(1)–N(2)	76.74(9)
<b>2</b>			
Cu(1)–O(1)	1.931(8)	O(1)–Cu(1)–O(2A)	92.50(15)
Cu(1)–O(2A)	1.991(3)	O(1)–Cu(1)–N(1)	168.07(15)
Cu(1)–O(3B)	2.085(3)	O(2A)–Cu(1)–N(1)	89.54(15)
Cu(1)–N(1)	2.004(4)	O(2A)–Cu(1)–N(2)	154.87(15)
Cu(1)–N(2)	2.039(4)	N(1)–Cu(1)–N(2)	80.71(15)
		O(1)–Cu(1)–O(3B)	91.94(15)
		N(1)–Cu(1)–O(3B)	99.86(15)

Symmetry transformations used to generate equivalent atoms: A  $x + 1/2, -y + 3/2, -z + 1/4$ ; B  $y - 1, x + 1, -z$  for **1**, A  $y + 1, x - 1, -z$ , B  $y + 1/2, -x + 3/2, z + 1/4$  for **2**.

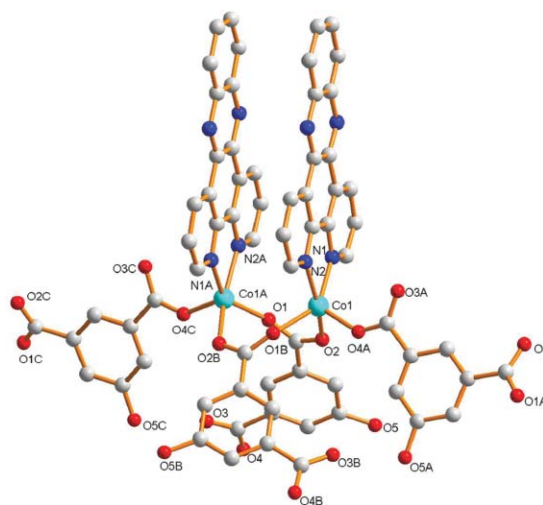


**Fig. 1** The  $[Co_2(DPPZ)_2(hip)_4]^{4+}$  second building unit assembled by four hip, two DPPZ and two Co(II) ions. Symmetry transformations used to generate equivalent atoms: A:  $x + 1/2, -y + 3/2, -z + 1/4$ ; B:  $y - 1, x + 1, -z$ ; C:  $-y + 1/2, x + 3/2, z - 1/4$ .

carboxylate oxygen atoms of the hip ligand are all deprotonated, and the two carboxylate groups of hip take different bridging patterns. One adopts a bridging bidentate coordination to connect two adjacent Co centres and the other adopts a monodentate coordination mode to one Co centre of the adjacent SUB. The adjacent Co(II) centres are connected by the bridging hip ligands to form the 1D left-handed helical chain along the  $b$ -axis with a pitch of 18.81  $\text{\AA}$  (Fig. 2a). There is also a  $2_1$  screw axis along the  $b$ -direction (the  $b$  axis is an equivalence of the  $a$ -axis in the tetragonal system), and a  $4_1$  screw axis in the  $c$ -direction, which contribute to the chirality of the compounds (Fig. 2b). As is known, helical structural motifs exhibit an axial chirality<sup>9</sup> and packing these 1D helical chains into a 3D chiral framework needs chiral discriminative interactions.<sup>10</sup> In **1**, the coordination bonds between the Co(II) centers and the hip linkers offer the chiral discriminative interactions that promote the chiral assembly.

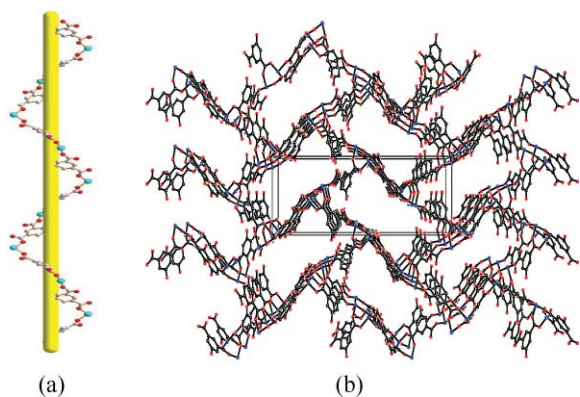


**Fig. 2** (a) The fragment of Co-hip-Co helical chain along the *b*-axis, (b) 3D metal-organic framework viewed along the *a*-axis, DPPZ ligands were omitted for clarity.

An interesting structural feature of the title compound shows that its structure reveals a new topology. If the binuclear Co2 is assigned as a node and the hip organic ligand as a linker, the framework of the title compound displays a 3D four-connected  $6^6$  topological net. Generally, the frameworks constructed from four connected tetrahedral nodes display diamond or diamond related nets,<sup>11</sup> where all the shortest circuits passing through one node are displayed as six-membered circuits with a chair form. It is interesting that the framework of the title compound did not display diamond or diamond-related nets. In the title compound, there are six six-membered circuits with a boat form (Fig. 3). Recently, the Feng group reported a novel compound,<sup>12</sup> Cu<sub>4</sub>I<sub>4</sub>(DABCO)<sub>4</sub> (DABCO = 1,4-diazabicyclo[2.2.2]octane), showing an interesting  $6^6$  topological net, in which there are five six-membered circuits with a boat form and one planar six-membered form.

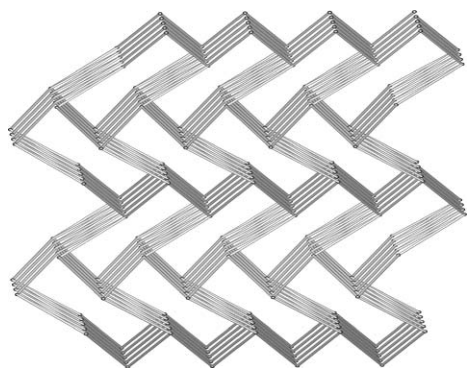


**Fig. 3** The topological representation of the 3D chiral metal-organic framework of **1** viewed along the *a*-axis.

Another attractive structural feature of **1** is that the 3D metal-organic framework possesses chirality. The value of the Flack parameter  $X = -0.01(2)$ . Fig. 4 shows the experimental VCD and IR spectra of the [Co(hip)(DPPZ)]<sub>n</sub> polycrystalline samples. The IR spectra of **1** are assigned as follows: the characteristic bands of carboxyl groups at 1608 and 1551 cm<sup>-1</sup> for the antisymmetric stretching and at 1495 and 1447 cm<sup>-1</sup> for symmetric stretching, the bands at 1413, 1384, 1356, 1219, 1297 cm<sup>-1</sup> are attributed to the skeleton vibrations of the aromatic ring. The experimental VCD bands at 1611–1594, 1562–1530 and 1510–1487, 1455–1441 cm<sup>-1</sup> correspond to the stretching vibrations of carboxyl groups, and the

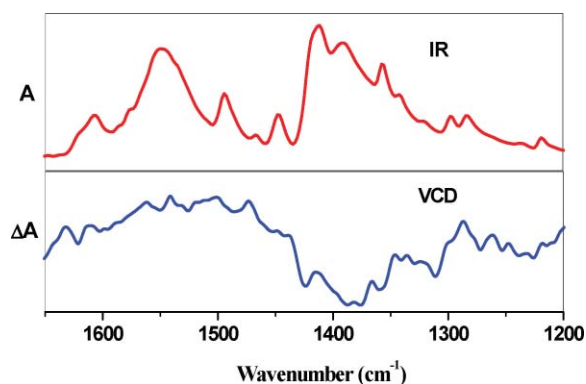


**Fig. 4** The IR absorption spectra (top) and VCD (bottom) of **1** in the solid state at room temperature.

bands at 1423–1244 cm<sup>-1</sup> correspond to the skeleton vibrations of the aromatic rings. The carboxyl group and the aromatic ring construct one type of Co-hip-Co helical chain. There is good agreement between the VCD and IR spectra. Each infrared absorption peak corresponded to a VCD feature, which could be either positive or negative. The relative intensities of the VCD bands could be greater or less than the relative intensities of their absorption bands. The vibrational modes were identified and conformational information can also be observed in the VCD spectra. The strong VCD signals show that the crystals of [Co(hip)(DPPZ)]<sub>n</sub> were not racemic. The experiment was repeated three times on compounds obtained from different independent syntheses.

To further investigate the absolute configurations of the two enantiomers, solid-state CD spectra of crystals synthesized in the same crystallization were measured.<sup>13</sup> As shown in Fig. 5, A and B are mirror images of one another and show different Cotton effects in the wavelength range of 200–500 nm, demonstrating the formation of either left-handed or right-handed enantiomers in a crystal, which confirms spontaneous resolution during the course of the crystallization. However, based on the CD measurement of 20 crystals from one crystallization (Fig. S3†), the enantiomeric excess *ee* ( $ee = 100 \times (A - B) / (A + B)$ ) value<sup>14</sup> for the crystallization is calculated to be *ca.* 60, also confirming that enantiomeric excess exists in the whole crystallization.

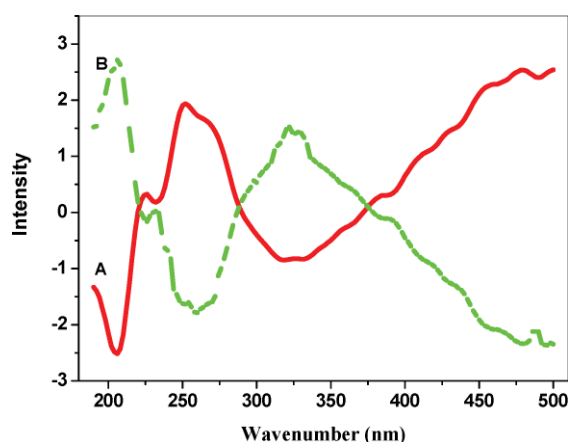


**Fig. 5** Solid-state CD spectra of crystals of compound **1** showing the contrasting cotton effects.

In order to understand the reason for the observed enantiomeric excess in the  $[\text{Co}(\text{hip})(\text{DPPZ})]_n$  product, we have checked all the reagents and solvents, and confirmed that we did not introduce any chiral stimulant during the synthetic procedure. Three independent syntheses from different experiments have been made and all crystals exhibited a similar VCD signal. The enantiomeric excess is unusual in spontaneous resolution and the reason may be explained by the fact that the initial crystals formed may seed the handedness of the bulk product in crystal growth, and thus the particular handedness of the bulk depends on which random hand is formed, which is similar to previously reported literature.<sup>15</sup>

The hydrothermal technique is widely used to prepare metal–organic compounds, and the mechanism is complex, many factors may influence the target compounds. In fact, the V-shaped dicarboxylate and the DPPZ ligands play a key role in the formation of the helical chains, in which the chirality is transferred into the whole three dimensional framework. Therefore, the design and selection of organic ligands is key in preparing chiral coordination complexes from achiral starting materials.

### IR spectra, XRPD patterns and thermogravimetric analyses

The absence of strong peaks around  $1700\text{ cm}^{-1}$  in **1** and **2** indicates that all carboxylic groups are deprotonated,<sup>16</sup> which is consistent with the results of the valence sum calculations. The simulated and experimental XRPD patterns of **1** and **2** are shown in Fig. S1.† Their peak positions are in good agreement with each other, indicating the phase purity of the products. The differences in intensity may be due to the preferred orientation of the powder samples.<sup>17</sup> The thermal stabilities of **1** and **2** were examined by TGA in a dry nitrogen atmosphere from 30 to 900 °C. The 3D framework of **1** was stable up to *ca.* 400 °C and then began to decompose upon further heating. The 3D framework of **2** was stable up to *ca.* 285 °C and then began to decompose upon further heating. (Fig. S2†).

### Magnetic properties

The thermal variations of  $\chi_m T$ , and  $1/\chi_m$  of **1** are displayed in Fig. 6a. The value of  $\chi_m T$  at room temperature is  $2.54\text{ cm}^3\text{ K mol}^{-1}$  per Co formula unit, which is larger than an uncoupled one ( $1.87\text{ cm}^3\text{ K mol}^{-1}$ ). Upon lowering the temperature,  $\chi_m T$  gradually decreases from  $2.54\text{ cm}^3\text{ K mol}^{-1}$  at 300 K to  $0.59\text{ cm}^3\text{ K mol}^{-1}$  at 2.0 K, indicating that an antiferromagnetic interaction exists predominantly between the Co(II) centers. The inverse susceptibility plot as a function of temperature is linear above 2 K, following the Curie–Weiss law with a Weiss constant,  $\theta = -2.77\text{ K}$ , and a Curie constant,  $C = 4.54\text{ cm}^3\text{ K mol}^{-1}$ . The larger  $\chi_m T$  value at room temperature and the larger Curie constant are the result of contributions to the susceptibility from orbital angular momentum.<sup>18</sup> The thermal variations of  $\chi_m T$ , and  $1/\chi_m$  of **2** are displayed in Fig. 6b. The value of  $\chi_m T$  at room temperature is  $0.388\text{ cm}^3\text{ K mol}^{-1}$  per Cu formula unit. Upon lowering the temperature,  $\chi_m T$  gradually decreases from  $0.388\text{ cm}^3\text{ K mol}^{-1}$  at 300 K to  $0.02\text{ cm}^3\text{ K mol}^{-1}$  at 2.0 K. The inverse susceptibility plot as a function of temperature is linear above 150 K, following the Curie–Weiss law with a Weiss constant,  $\theta = -2.82\text{ K}$ , and a Curie constant,  $C = 0.39\text{ cm}^3\text{ K mol}^{-1}$ , indicating that an antiferromagnetic interaction exists between the Cu(II) centers.

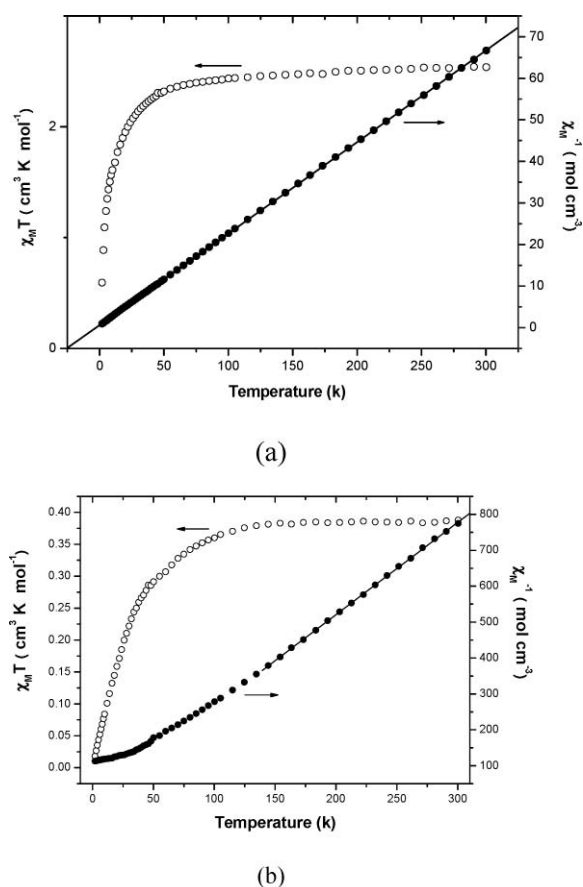


Fig. 6 Plot of  $\chi_m T$ ,  $\chi_m^{-1}$  versus  $T$  for the polycrystalline samples of **1** (a) and **2** (b) with solid lines showing the Curie–Weiss fitting curves.

### Conclusions

In summary, we have developed a synthetic strategy toward 3D chiral coordination frameworks with helical chains by using a V-shaped ligand, DPPZ and a transition metal ion. This work provides a good route for further exploration of the preparation of optical coordination polymers and other aesthetic structural motifs. The investigation of other transition metal ions/V-shaped dicarboxylates system is underway.

### Acknowledgements

This work was supported by the National Natural Science Foundation (20871063) and the Program for Liaoning Excellent Talents in University (RC-05-11).

### References

- (a) L. Q. Ma, C. Abney and W. B. Lin, *Chem. Soc. Rev.*, 2009, **38**, 1248; (b) S. J. Lee and W. B. Lin, *Acc. Chem. Res.*, 2008, **41**, 521; (c) O. M. Yaghi, M. O’Keeffe, N. W. Ockwig, H. K. Chae, M. Eddaoudi and J. Kim, *Nature*, 2003, **423**, 705; (d) S. Kitagawa, R. Kitaura and S. Noro, *Angew. Chem., Int. Ed.*, 2004, **43**, 2334; (e) D. X. Xue, W. X. Zhang, X. M. Chen and H. Z. Wang, *Chem. Commun.*, 2008, 1551.
- (a) G. Li, W. B. Yu, J. Ni, T. F. Liu, Y. Liu, E. H. Sheng and Y. Cui, *Angew. Chem., Int. Ed.*, 2008, **47**, 1245; (b) Y. Liu, X. Xu, F. K. Zheng and Y. Cui, *Angew. Chem., Int. Ed.*, 2008, **47**, 4538; (c) G. Li, W. B. Yu and Y. Cui, *J. Am. Chem. Soc.*, 2008, **130**, 4582; (d) J. S. Seo, D. Whang, H. Lee, S. I. Jun, J. Oh, Y. J. Jeon and K. Kim, *Nature*, 2000, **404**, 982;

- (e) G. Cao, E. G. Maurie, A. Monica, F. B. Lora and E. M. Thomas, *J. Am. Chem. Soc.*, 1992, **114**, 7574; (f) S. J. Lee, A. G. Hu and W. B. Lin, *J. Am. Chem. Soc.*, 2002, **124**, 12948; (g) E. M. Thomas and A. G. Julia, *Acc. Chem. Res.*, 1998, **31**, 209.
- 3 (a) C. D. Wu and W. B. Lin, *Angew. Chem., Int. Ed.*, 2005, **44**, 1958; (b) H. Y. An, E. B. Wang, D. R. Xiao, Y. G. Li, Z. M. Su and L. Xu, *Angew. Chem., Int. Ed.*, 2006, **45**, 904; (c) X. Shi, G. S. Zhu, S. L. Qiu, K. L. Huang, J. H. Yu and R. R. Xu, *Angew. Chem., Int. Ed.*, 2004, **43**, 6482; (d) J. Zhang and X. H. Bu, *Chem. Commun.*, 2008, 1756; (e) D. N. Dybtsev, A. L. Nuzhdin, H. Chun, K. P. Bryliakov, E. P. Talsi, V. P. Fedin and K. Kim, *Angew. Chem., Int. Ed.*, 2006, **45**, 916.
- 4 (a) Z. J. Lin, A. M. Z. Slawin and R. E. Morris, *J. Am. Chem. Soc.*, 2007, **129**, 4880; (b) J. Zhang, S. M. Chen, T. Wu, P. Y. Feng and X. H. Bu, *J. Am. Chem. Soc.*, 2008, **130**, 12882; (c) D. Bradshaw, T. J. Prior, E. J. Cussen, J. B. Claridge and M. J. Rosseinsky, *J. Am. Chem. Soc.*, 2004, **126**, 6106; (d) J. Zhang, R. Liu, P. Y. Feng and X. H. Bu, *Angew. Chem., Int. Ed.*, 2007, **46**, 8388.
- 5 (a) B. Kesanli and W. B. Lin, *Coord. Chem. Rev.*, 2003, **246**, 305; (b) L. Pérez-García and D. B. Amabilino, *Chem. Soc. Rev.*, 2002, **31**, 342; (c) Y. T. Wang, M. L. Tong, H. H. Fan, H. Z. Wang and X. M. Chen, *Dalton Trans.*, 2005, 424; (d) J. D. Ranford, J. J. Vittal, D. Wu and X. Yang, *Angew. Chem., Int. Ed.*, 1999, **38**, 3498; (e) T. Ezuhara, K. Endo and Y. Aoyama, *J. Am. Chem. Soc.*, 1999, **121**, 3279; (f) K. Biradha, C. Seward and M. J. Zaworotko, *Angew. Chem., Int. Ed.*, 1999, **38**, 492.
- 6 (a) M. Kondo, M. Miyazawa, Y. Irie, R. Shinagawa, T. Horiba, A. Nakamura, T. Naito, K. Maeda, S. Utsuno and F. Uchida, *Chem. Commun.*, 2002, 2156; (b) E. Q. Gao, Y. F. Yue, S. Q. Bai, Z. He and C. H. Yan, *J. Am. Chem. Soc.*, 2004, **126**, 1419.
- 7 (a) F. M. Tabellion, S. R. Seidel, A. M. Arif and P. J. Stang, *Angew. Chem., Int. Ed.*, 2001, **40**, 1529; (b) M. Sasa, K. Tanaka, X. H. Bu, M. Shiro and M. Shionoya, *J. Am. Chem. Soc.*, 2001, **123**, 10750.
- 8 G. M. Sheldrick, *SHELXTL*, Version 6.10, Bruker Analytical X-ray Systems, Madison, WI, USA, 2001.
- 9 P. A. Maggard, C. L. Stern and K. R. Poeppelmeier, *J. Am. Chem. Soc.*, 2001, **123**, 7742.
- 10 Q. Shi, R. Cao, D. F. Sun, M. C. Hong and Y. C. Liang, *Polyhedron*, 2001, **20**, 3287.
- 11 S. R. Batten and R. Robson, *Angew. Chem., Int. Ed.*, 1998, **37**, 1460.
- 12 M. H. Bi, G. H. Li, Y. C. Zou, Z. Shi and S. H. Feng, *Inorg. Chem.*, 2007, **46**, 604.
- 13 A. Beghidja, P. Rabu, G. Rogez and R. Welter, *Chem.–Eur. J.*, 2006, **12**, 7627.
- 14 Q. Z. Sun, Y. Bai, G. J. He, C. Y. Duan, Z. H. Lin and Q. J. Meng, *Chem. Commun.*, 2006, 2777.
- 15 (a) Y. Ma, Z. B. Han, Y. K. He and L. G. Yang, *Chem. Commun.*, 2007, 4107; (b) Z. B. Han, Y. K. He, M. L. Tong, Y. J. Song, X. M. Song and L. G. Yang, *CrystEngComm*, 2008, **10**, 1070; (c) G. Tian, G. S. Zhu, X. Y. Yang, Q. R. Fang, M. Xue, J. Y. Sun, Y. Wei and S. L. Qiu, *Chem. Commun.*, 2005, 1396.
- 16 Z. B. Han, Y. K. He, C. H. Ge, J. Ribas and L. Xu, *Dalton Trans.*, 2007, 3020.
- 17 A. Gilbert, and J. Baggott, *Essentials of Molecular Photochemistry*; CRC Press, Boca Raton, FL, 1991; pp 87-89.
- 18 Y. Q. Xu, D. Q. Yuan, B. L. Wu, L. Han, M. Y. Wu, F. L. Jiang and M. C. Hong, *Cryst. Growth Des.*, 2006, **6**, 1168.